

J. A. Wang<sup>1</sup> and N. S. Rao<sup>1</sup>

## **New Methodologies for Developing Radiation Embrittlement Models and Trend Curves of the Charpy Impact Test Data**

---

**Reference:** J. A. Wang and N. S. Rao, "New Methodologies for Developing Radiation Embrittlement Models and Trend Curves of the Charpy Impact Test Data," *Effects of Radiation on Materials, ASTM STP 1447*, M. L. Grossbeck, Ed., ASTM International, West Conshohocken, PA, 2003.

**Abstract:** A new methodology is developed for the prediction of RPV embrittlement that utilizes a combination of domain models and nonlinear estimators including neural networks and nearest neighbor regressions. The Power Reactor Embrittlement Database is used in this study. The results from newly developed near neighbor projective fuser indicate that the combined embrittlement predictor achieved about 67.3% and 52.4% reductions in the uncertainties for General Electric Boiling Water Reactor plate and weld data compared to Regulatory Guide 1.99, Revision 2, respectively. The implications of irradiation temperature effects to the development of radiation embrittlement models are then discussed. A new methodology that incorporates the chemical compositions into the Charpy trend curve was also developed. The purpose of this new fitting procedure is to generate a new multi-space topography that can properly reflect the inhomogeneity of the surveillance materials and utilize this multi-space trend surface to link and project the surveillance test results to that of reactor pressure vessel steels.

**Keywords:** Radiation Embrittlement, Reactor Vessel Integrity, Information Fusion, Power Reactor, Boiling Water Reactor, Material Modeling, Charpy Curve Fitting.

### **Introduction**

The success of reactor technology depends critically on an effective surveillance program to monitor the degradation of irradiated materials during service. The aging and degradation of light-water Reactor Pressure Vessels (RPVs) are of particular concern because the magnitude of the radiation embrittlement is extremely important to the plant's safety and operating cost. Property changes in materials due to neutron-induced displacement damage are a function of neutron flux, neutron energy, and temperature, as well as the pre-irradiation material history, material chemical composition and microstructure, since each of these influence radiation-induced microstructural evolution. These factors must be considered to reliably predict RPV embrittlement and to ensure the

---

<sup>1</sup> Research Scientist, Oak Ridge National Laboratory, P.O. Box 2008, Oak Ridge, TN 37831.

structural integrity of the RPV. Based on the embrittlement predictions, decisions must be made concerning operating parameters, low-leakage-fuel management, possible life extension, and the potential role of pressure vessel annealing. Therefore, the development of embrittlement prediction models for nuclear power plants (NPPs) is a very important issue for the nuclear industry regarding the safety and lifetime extension of aging commercial nuclear power plants.

Service failures due to inaccurate characterization of material aging responses could result in potentially costly repairs or premature component replacements, and in a worst-case could result in a catastrophic failure and loss of life. The general degradation mechanisms of the material aging behavior can be quite complicated and include: microstructure and compositional changes, time-dependent deformation and resultant damage accumulation, environmental attack and the accelerating effects of elevated temperature, and synergistic effects of all the above. These complex nonlinear dependencies make the modeling of aging material behaviors a difficult task.

There have been several domain models that capture various aspects of material behavior; these models are designed by the domain experts to capture various critical relationships. At the same time, conventional non-linear estimators - while requiring very limited domain expertise - can model relationships that are not readily apparent. Consequently, there has been a profusion of methods with complementary performance with no single method proven to be always better than all others. Our goal is to develop an effective methodology by combining the domain models with the nonlinear estimators including, neural networks and nearest neighbor regressions to exploit their complementary strengths.

We have previously developed a large Power Reactor Embrittlement Database (PR-EDB) [1] for U.S. nuclear power plants. Subsequently in cooperation with the Electric Power Research Institute, additional verification and quality assurance of the data were performed by the U. S. reactor vendors. PR-EDB is used in this study to predict the embrittlement levels in light water reactor pressure vessels. The results from newly developed near neighbor projective fuser indicate that our combined predictor achieved about 67.3% and 52.4% reductions in the embrittlement uncertainties for General Electric Boiling Water Reactor plate and weld data compared to Regulatory Guide 1.99, Revision 2, respectively.

A new methodology that incorporates the chemical compositions into the Charpy trend curve was also developed. The purpose of this new fitting procedure is to generate a new multi-space topography that can properly reflect the inhomogeneity of the surveillance materials and utilize this multi-space trend surface to link and project the surveillance test results to that of reactor pressure vessel steels.

## **Charpy Data Fitting Procedures**

The current practice of Charpy curve-fitting procedures used in PR-EDB is based on the hyperbolic tangent model [2], which has been proven to be successful for the determination of transition temperature for materials which have more or less homogeneous properties. The impact energy and testing temperature are used as the two

primary input parameters for the determination of the fitting curve. The hyperbolic tangent model relates impact energy E to the test temperature T according to the formula

$$E = \left\{ \left( \frac{USE + LSE}{2} \right) + \left( \frac{USE - LSE}{2} \right) * \text{Tanh} \left[ \text{SLOPE} (T - T_M) \right] \right\}, \quad (1)$$

with USE and LSE the upper- and lower-shelf energy, respectively, with  $T_M$  as the midpoint of the transition temperature region, and SLOPE as the slope of the curve at  $T_M$ . This model is purely phenomenological but well characterizes the general shape of a Charpy curve in terms of the four basic parameters, USE, LSE,  $T_M$ , and SLOPE. The hyperbolic tangent function is the most widely used fitting procedure next to hand (eyeball) fitting.

For a particular raw Charpy data set provided with chemistry information for each individual specimen, if certain data exhibit a large degree of scatter about the best-fit line, detailed study from PR-EDB [1] shows that these data generally either have a much higher copper or lower copper content than the rest of the specimens. This may imply that when the greater inhomogeneity of specific test sets are known, further constraints need to be added into the Charpy curve-fitting model, such as copper and nickel contents, to allow for material inhomogeneity.

#### *Characterization of Surveillance Charpy Impact Test Data*

Surveillance Charpy impact data scatter is the result of the inhomogeneity of the materials, physical location and position of test specimens from the RPV plates, material history, inherited mechanical testing, and other factors due to service environment, etc. In general, the impact energy of the Charpy impact test samples from RPV surveillance capsules depends on irradiation temperature, neutron fluence, and chemical compositions and material history of the test samples, which can be described as below.

$$E = f(T, \mathbf{j}t, Cu, Ni, \text{Material History}, \text{Microstructure}, \dots)$$

Fluence and irradiation time are generally treated as constant for data within the same capsule, and RPV materials, such as base, weld and HAZ, are categorized within separated groups; thus, the impact of microstructure factor can be minimized. Therefore, the formulation of the impact energy for a Charpy impact data set from one surveillance capsule can be further simplified and written as follows:

$$E = f(T, Cu, Ni, \dots)$$

For each individual Charpy data, impact energy can be written as

$$E_i = f(T_i, Cu_i, Ni_i, \dots)$$

#### *Proposed New Fitting Function with Consideration of the Chemistry Variability*

In order to consider the chemical variability of the surveillance test samples, a new fitting procedure that incorporates the chemical composition into the governing equation was developed. The formula for the impact energy as a function of test temperature (T), and Cu and Ni (or plus other chemistry, such as P, Mn, etc.) can be written as below:

$$E = \left\{ A + B * \text{Tanh} \left[ \frac{T - T_M}{C} \right] \right\} * f(Cu, Ni, \dots) \quad (2)$$

The preliminary testing function of function  $f$ , for Cu and Ni contents, can be written as follows:

$$f(Cu, Ni) = C_5 * Cu + C_6 + C_7 * \sqrt{Cu * Ni} ,$$

where  $A=(USE+LSE)$ ,  $B=(USE-LSE)$ ,  $C=1/SLOPE$ ,  $C_i$  are constant fitting parameters. This approach assumes that there is no major change of the general trend between the new fitting equation and the conventional fitting curve without the consideration of chemical variability.

This new fitting procedure provides a new multi-dimension topography that can properly reflect the inhomogeneity of the surveillance materials.

### Advanced Charpy Data Fitting Function

A more sophisticated formulation of the proposed new fitting procedure that takes into account the shape change of the hyperbolic tangent fit curve was developed and is illustrated below.

$$E = \left\{ A + B * \text{Tanh} \left[ \frac{T - T_0 / f_1}{C * / f_2} \right] \right\} * f_3 + f_4 , \quad (3)$$

where,  $f_i$ ,  $i=1,4$ , are functions of chemical compositions for Cu and Ni contents, which are written as follows,

$$f_1 = C_8 * Cu, \quad f_2 = C_9 * Cu, \quad f_3 = C_{10} * (Cu * Ni) + C_{11}$$

$$f_4 = C_5 * C + C_6 * \sqrt{Cu * Ni} + C_7$$

where,  $C_i$ ,  $i=5, 11$ , are constant-fitting parameters.

### Results of the Proposed Fitting Procedures

The weld Charpy data, with HEAT\_ID = WDR301 listed in PR-EDB, from surveillance capsule 18 of Dresden Unit 3 nuclear power plant were used for this feasibility study.

*Conventional Hyperbolic Tangent Fit Result* – Equation 1 was used in the curve fitting, where IMSL routine ZXSSQ was used in the non-linear least squares fitting evaluation to determine the constant fitting parameters. Which give the one standard deviation as 13.84°C for the selected WDR301 surveillance data set. The estimated constant-fitting parameters are  $A=50.85$  J,  $B= 47.85$  J,  $T_M=15^\circ\text{C}$ , and  $SLOPE = 0.0179$ . The corresponding hyperbolic tangent fitting curve and data are shown in Fig. 1.

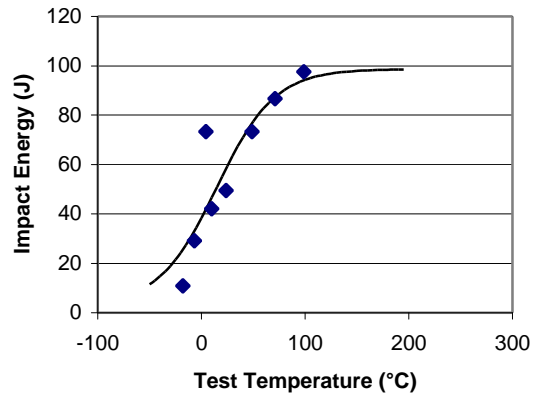


Fig. 1. Charpy data of Dresden Unit3 Capsule 18 WDR301 in TL Orientation.

*New Fitting Function Test Results* – A FORTRAN program was written for this feasibility study, where IMSL routine ZXSSQ was used in the non-linear least squares fitting. Based on equation 2, the estimated one standard deviation is 12.09°C, the average chemistry of Cu and Ni are 0.2077 and 0.353 wt%, respectively. The estimated constant-parameters are listed below.

A= 50.85 J, B=47.85 J,  $T_M=8.0^\circ\text{C}$ , and SLOPE = 0.0379, C5 =15.09, C6=2.869, and C7=-18.5.

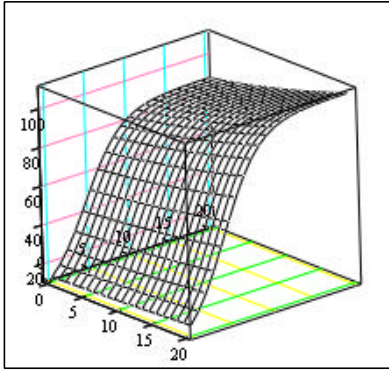


Fig. 2. 3-D plot of Eq. 2, with Ni fixed at average, 0.353wt

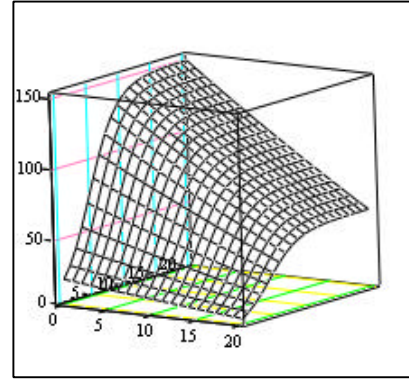
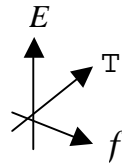


Fig. 3. 3-D plot of Eq. 2 with Cu fixed at average, 0.2077wt

*Advanced Testing Function Fit Results* – Based on equation 3, the estimated one standard deviation is 10.05°C, the average chemistry of Cu and Ni are 0.2077 and 0.353 wt %, respectively. The estimated constant-parameters are listed below.

A=50.3 J, B= 47.3 J,  $T_0=5.87^\circ\text{C}$ , and Slope = 0.00805, C5 =1032, C6=-123, C7=-277.4, C8=1.566, C9=1.987, C10=-25.47, and C11=2.891.

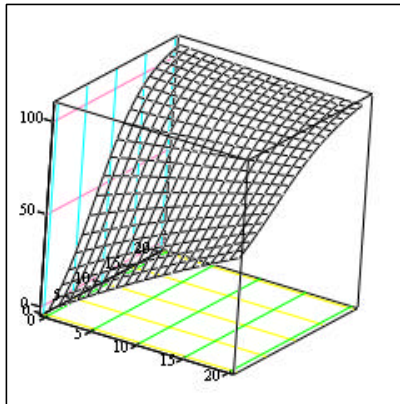


Fig. 4. 3-D plot of Eq. 3, with Ni fixed at average, 0.353wt %.

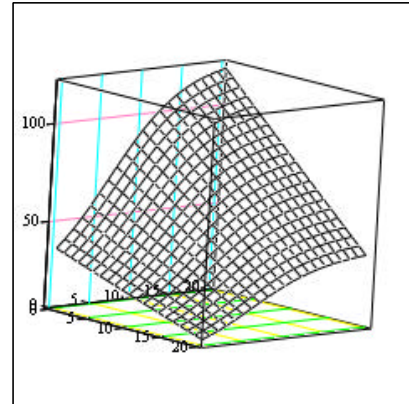
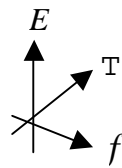


Fig. 5. 3-D plot of Eq. 3 with Cu fixed at average, 0.2077wt

*Applying New Fitting Procedure for Surrogate Material Research*

Based on the proposed new fitting procedure, a multi-dimension topography can be generated. For simplification, one uses the 3-D Cartesian coordinate to illustrate the developed multi-dimension topography (see Fig. 6), where test temperature and impact energy stand for the x and z-coordinates, respectively, and the third axis represents the integrated formulation of the chemistry composition functions,  $f_i$ .

*Evaluation of the Trend Curve for the Target Chemistry Data –*

Based on constructed multi-space topography, as illustrated in Fig. 6, one can substitute the target chemistry into a new Charpy fitting equation and develop a new trend curve for the target materials. Therefore, this new procedure provides an expedient way to determine trend curve for the surrogate materials of the RPV surveillance program. Furthermore, based

on this new approach, the new advanced fitting procedure achieves a reduction in uncertainty by 27%, compared to that of conventional hyperbolic tangent fit procedure. However, caution should be exercised while using these fitting functions, due to high-order nonlinearity, and chemistry of the target materials should be within one-standard deviation of the mean chemistry from which the new fitting equation was developed.

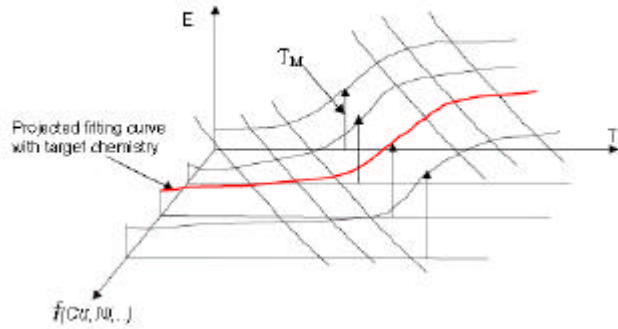


Fig. 6. Illustration of projected trend curve.

**New Methodologies for Developing Radiation Embrittlement Models**

*Background*

The complex nonlinear dependencies observed in typical material embrittlement data, as well as the existence of large uncertainties and data scatter, make the modeling of material behavior (such as embrittlement prediction) a difficult task. The conventional statistical and deterministic approaches have proven to result in large uncertainties, in part because they do not fully exploit the domain specific knowledge. The domain models built by researchers in the field, on the other hand, are not able to fully exploit the statistical and information content of the data. As evidenced in previous studies, it is unlikely that a *single* method, whether it is statistical, non-linear or domain model will outperform all others. Considering the complexity of the problem, it is more likely that certain methods will perform best under certain conditions. In this paper, we propose to combine a number of methods such as domain models, neural networks, and nearest neighbor regressions. The combined system has the potential to perform at least as well as the best of the constituents by exploiting the regions where the individual methods are superior. Such a combination of methods became possible due to recent developments in measurement-based optimal fusers [3-5] in the area of information fusion.

The problem of estimating nonlinear relationships from noisy data has been well studied in the area of statistical estimation [6]. The nonlinear statistical estimators such as the Nadaraya-Watson estimator and regressograms [7] essentially rely on the properties of regressions. While neural networks and statistical estimators are general, the domain models developed by the material scientists specifically capture the critical relationships in the data that are not easily amenable to general methods. Such models are typically based on a combination of linear and nonlinear models, which are carefully chosen through an understanding of experimental data.

Particularly among the models developed for embrittlement data, there is unlikely to be a single winner, and different models perform well under different conditions. By discarding one or more models, one stands the risk of not characterizing certain critical performance. We propose to combine various methods using isolation fusers [6]. The most important part of these fusers is that the combined system can be guaranteed to be at least as good as the best individual estimator with a specified probability. Furthermore, fusion of no proper subset of the models performs better than the fused system based on all models. This way the positive aspects of *all* individual estimators can be exploited without discarding any single estimator. The deployment of these fusers on various models will ensure that the fused model is at least as good as the best of the individual models, irrespective of their individual performances. However, the general results on fusers do not specify the actual performance gains that may be achieved in a particular application. We show here that significant performance improvements are indeed obtained by employing fusers to combine various embrittlement models.

### *Approach*

We employ neural networks, nearest neighbor regressions, and domain models, based on the PR-EDB data, to predict the transition temperature shift of RPV materials, which is a measure of the material embrittlement. From past experience [8], the boiling water reactor data has larger uncertainty compared to the other power reactor data. In this study, we only focused on the boiling water reactor data.

The first task is to create unbiased training and test sets. The General Electric (GE) boiling water reactors' (BWR) surveillance data (listed in PR-EDB) were preprocessed and streamlined. The final processed GE BWR data were compared with that of the ASTM E10.02 subcommittee embrittlement database for consistency in the surveillance information, such as irradiation temperature, chemical composition, Charpy impact test data fitting methodology, and power time history, etc. The processed GE BWR data has essentially the same neutron fluences, chemistry, and irradiation temperature data compared to that of ASTM E10.02 database, with minor difference of transition temperature shift (within a few degree F). The GE BWR's data values were then scaled to the interval [-1, 1] using a Linear Max/Min transformation. This ensures that no one component in the data dominates the parameter optimization scheme. Then the data were randomly partitioned into training and testing sets.

The second task consists of determining a number of estimators for this problem. For each method, a criteria function and optimization routine will be selected that consistently produces stable results. For statistical estimators, we will follow the

procedure described in the literature. For artificial neural networks (ANN), one hidden layer and eleven hidden nodes were chosen with 2000 epoch iteration. A random generator was used to generate the initial weights for ANN modeling. Four sets of ANN models were tested. We then combine the statistical and deterministic estimators using information fusion techniques.

An optimal projective fuser [4] proposed earlier was based on the lower envelope of error regressions of the estimators. In most practical cases, however, the error regressions are not available and only a finite sample is given. Consequently this fuser is hard to implement and furthermore provides only asymptotic consistency. In this paper, we propose a projective fuser based on the nearest neighbor concept [9], which is easy to implement. The combined system is guaranteed to perform at least as well as the best of the constituents by exploiting the regions where the individual methods are superior.

A novel methodology is developed here for inferring nonlinear relationships that are typical in material behavior prediction. A tool based on this methodology is also implemented for the embrittlement prediction of NPPs. This tool could be expanded and adapted for use in other areas in which nonlinear material properties are important, such as failure analysis of an earthquake event, airplane safety analyses, and others.

### *Embrittlement Prediction Models*

In this section we briefly described various models used for embrittlement prediction, which will be combined in the next section.

*ORNL Embrittlement Prediction Models* – The residual defects in materials due to neutron induced-displacement damage are a function of neutron energy, neutron flux, exposure temperature, and the material properties that determine how neutrons interact with atoms and how defects interact within the material [10]. Thus, temperature, neutron flux, neutron energy spectrum, and material composition and processing history all contribute to the radiation embrittlement process [11]. Insufficient consideration of these factors may result in misleading correlations and, thus, incorrect predictions of material state and material behavior, as well as incorrect end-of-life determinations.

The development of new embrittlement prediction equations [8,12] stem from a series of studies on radiation embrittlement models, such as Guthrie's model [11], Odette's model [14], Fisher's model [15], B&W Lowe's model [16], the French FIM model [17], etc., and several other parameter studies on the PR-EDB. Although the copper-precipitation model has been extremely successful in explaining many aspects of irradiation embrittlement, it is becoming increasingly evident that other elements also contribute to the embrittlement of the RPV steel, such as Ni, P, Mn, Mo, and S. Theoretically, all the impurities in low alloy steel are candidates to be included in the modeling. For example, C, Si, Mn, Mo, S, etc., were investigated in the test run, but including or excluding these elements did not affect the overall outcome of the statistical parameters significantly; therefore, these parameters (or elements) were not incorporated into final governing equations. Thus, Cu, Ni, and P were tentatively selected as key elements and were incorporated into the formula of the new prediction equations. Furthermore, the reason for separating weld and base metals is because the welds tend to



show enhanced degradation, the welding process presents a possible region of physical and metallurgical discontinuity, and offers added chances for the introduction of defects and undesirable components or stresses.

A nonlinear-least-squares fitting Fortran program was written for this study. The development of the parameters for this new embrittlement model is based on statistical formulation chosen by computer iterations. To some extent, the physical mechanisms are embedded in the equations, such as the formulation of the fluence factor. Two new prediction models for the GE BWR data were developed, where the fluence rate effect was considered in the second prediction model and are described below:

Model 1:

$$\begin{aligned}\Delta RTNDT(Base) &= [-94.8 + 411.9Cu + 247.3\sqrt{CuNi} + 498P/Cu]f^{0.3216 - 0.001003\ln f} \\ \Delta RTNDT(Weld) &= [420.9Cu + 134.6\sqrt{CuNi} - 25.94P/Cu]f^{0.2478 - 0.01475\ln f}\end{aligned}\quad (4)$$

Model 2

$$\begin{aligned}\Delta RTNDT (Base) &= \left[ (13.62 + 318.1Cu - 58.75\sqrt{NiCu} - 151.4 P / Cu) f^{-0.4354 - 0.1285 \ln f} \right] \\ &\quad + \left[ (18.44 - 49.13\sqrt{CuNi} - 17.22Cu - 97.57P / Cu) f (-8.344 - 0.7045 \ln f) \ln(t_i / 600000) \right] \\ \Delta RTNDT (Weld) &= 1.075 \left[ (1580Cu - 86.06\sqrt{NiCu} + 43.55 P / Cu) f^{0.6523 + 0.02866 \ln f} \right] \\ &\quad - 2.23 \left[ (4.193 Ni - 45.54 Cu) f (-11.63 - 0.4554 \ln f) \ln(t_i / 600000) \right]\end{aligned}\quad (5)$$

where  $\Delta RTNDT$  is the transition temperature shift in °F; and neutron fluence  $f$  is in unit of  $10^{19}$  n/cm<sup>2</sup> ( $E > 1$  MeV), effective full power time,  $t_i$ , is in hour, and Cu, Ni, P. are in wt %. The residuals, defined as “measured shift minus predicted shift,” for ORNL Model2 are illustrated in Figs. 7-8 for base and weld, respectively.

*Regulatory Guide 1.99, Revision 2's Model* – The transition temperature shift of Reg. Guide 1.99, Rev. 2's model [18] was also used in this study for comparison, which is described as below.

$$\Delta RT_{NDT} = (CF) f^{(0.28 - 0.10 \log f)} \quad (6)$$

where,  $\Delta RT_{NDT}$  is the transition temperature shift in °F, CF(°F) is the chemistry factor (given in the Table 1 and Table 2 of Reg. Guide 1.99, Revision 2), which is a function of copper and nickel content, and neutron fluence  $f$  is in unit of  $10^{19}$  n/cm<sup>2</sup> ( $E > 1$  MeV).

The residuals for Reg. Guide 1.99, Rev. 2's model are illustrated in Figs. 9-10 for base and weld, respectively.

*Eason's Models* – The developed embrittlement model by E. D. Eason et. al. (Eason's model) [19], was used in this study. The Eason's trend curve of transition temperature shift was developed based on the power reactor data, and is described below. The residual of Eason's model are illustrated in Figs. 11-12 for base and weld, respectively.

$$\Delta T_{3op} = ff_1(\mathbf{f}t) + ff_2(\mathbf{f}t) f(cc), \quad [^{\circ}F]$$

$$ff_1(\mathbf{f}t) = A \cdot \exp\left[\frac{1.906 \cdot 10^4}{T_c + 460}\right] (I + 57.7 P) \left[\frac{\mathbf{f}t}{10^{19}}\right]^a$$

$$ff_2(\mathbf{f}t) = \frac{I}{2} + \frac{I}{2} \tanh\left[\frac{\log(\mathbf{f}t + 5.48 \cdot 10^{12} t_i) - 18.29}{0.600}\right]$$

$$ff(cc) = B(Cu - 0.72)^{0.682} (I + 2.56 Ni^{1.358}) \quad (7)$$

where,  $a = 0.4449 + 0.0597 \cdot \log\left[\frac{\mathbf{f}t}{10^{19}}\right]$ ,  $\mathbf{f}t$  = fluence

Welds :  $A = 1.10 \cdot 10^{-7}$ ,  $B = 209$ , Plates :  $A = 1.24 \cdot 10^{-7}$ ,  $B = 172$

Forgings :  $A = 0.90 \cdot 10^{-7}$ ,  $B = 135$ ,  $T_c$  is coolant inlet temperature,  $^{\circ}F$

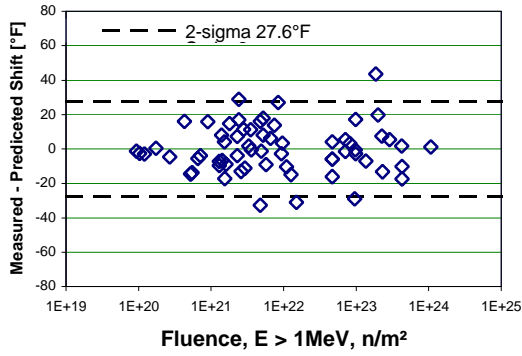


Fig. 7. ORNL Model 2 base residuals.

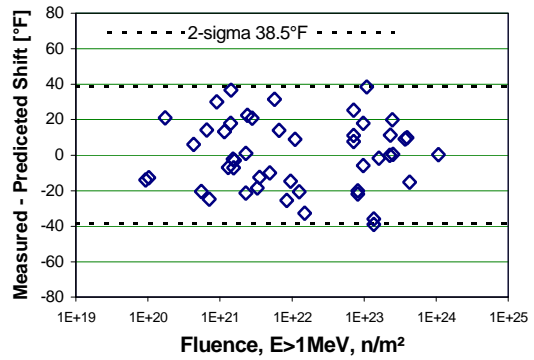


Fig. 8. ORNL Model 2 weld residuals.

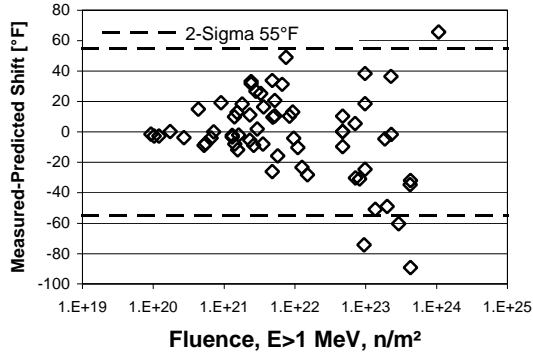


Fig. 9. R.G. 199/R2 base residuals.

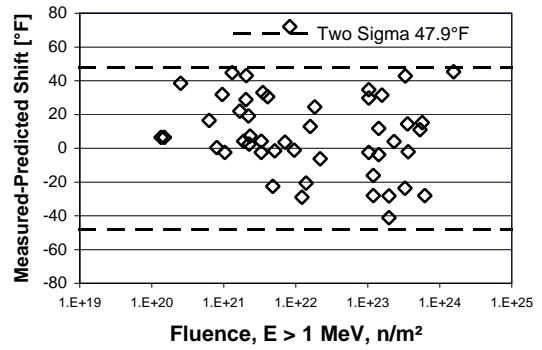


Fig. 10. R.G. 199/R2 weld residuals.

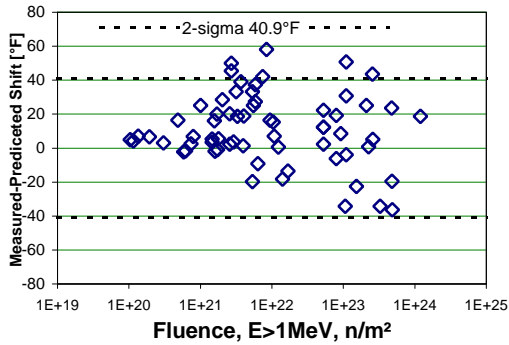


Fig. 11. Eason Model base residuals.

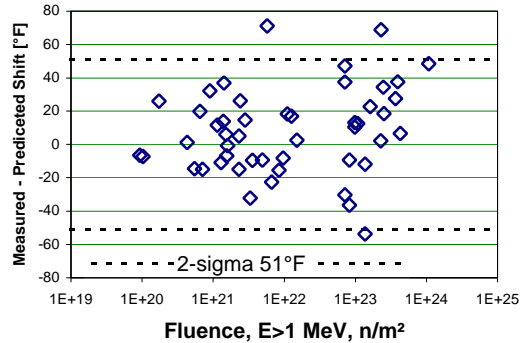


Fig. 12. Eason Model weld residuals.

*ANN Models* – An ANN is a parameterized nonlinear mapping from an input space to an output space [20]. An ANN realizes mapping from an m-dimensional input space to an n-dimensional output space and will have m nodes in its input layer and n nodes in its output layer. A multi-layer ANN (ML-ANN) is the most common architecture. This architecture has additional layers of nodes between the input and output layers. The information from each input-layer node is fanned out to nodes in the layer hidden between the input and output layers. The information entering a node in any hidden or output layer is the weighted sum of all information leaving the layer below it in the hierarchy. The node performs a non-linear/sigmoidal transformation on the weighted information it receives and fans out the result to all nodes in the layer above it in the hierarchy (except for the output layer). The weighting factors (weights) are free parameters that must be adjusted to some chosen criteria function using some optimization algorithm. In this way, ANNs are able to capture many higher-order correlations that may exist in the data. The relationship between the higher-order correlations produces a nonlinear mapping. This is the reason ANNs may offer a more accurate prediction of material behaviors, embrittlement in this case. With methods like ANNs, one has a better tool to extract nonlinear relationships from embrittlement data to aid in the development of reliable maintenance and safety strategies and regulations in the nuclear industry.

The backpropagation algorithm is used to train the network with the data [20]. The training process determines the weights of ANN to fit a suitable nonlinear map. The backpropagation's flexibility in training an ANN is why it does a better job of modeling than linear regression, but this method has several weaknesses. The backpropagation algorithm is based on local descent and can get stuck in local minima, and as a result the predictive properties can be quite varied. Also, there are a number of tunable parameters such as starting weights and learning rates that have a significant effect on the weight computed by the backpropagation algorithm. Thus, when different ANN models are trained with the same backpropagation algorithm but with different starting weights and learning rates, the performance can be significantly different. These networks however can be fused to achieve the performance of the best ANN [4] creating a more robust architecture.

Six independent variables, namely, Cu, Ni, P, fluence, irradiation temperature, and effective full power time were used in the ANN models. A program written in C language was used in this study.

*K-Nearest Neighbor Regression (K-NNR) Method* – The nearest neighbor regression (NNR) [6] is also chosen to generate an embrittlement model. The algorithm is described below. Let  $x_1, x_2, x_3, \dots, x_n$  be a sequence of n independent measurements with known classifications, and  $x$  be the measurement to be classified. Among  $x_1, x_2, x_3, \dots, x_n$ , let the measurement with the smallest distance from  $x$  be denoted as  $x'$ . Then the nearest-neighbor decision rule assigns the classification of  $x'$  to that of  $x$ . As for K-NNR, it assigns to an unclassified sample point the class most heavily represented among its K nearest neighbors to  $x$ . In this study we chose the first three nearest neighbors with properly weighted function to represent the unclassified sample.

Six independent variables, namely, Cu, Ni, P, fluence, irradiation temperature, and effective full power time were used in K-NNR models. A second test K-NNR model, excluding irradiation temperature from the fitting parameter, generated a nearly identical trend curve as that with irradiation temperature. A program written in C language was used in this study.

### *Fusion of Embrittlement Models*

The development of this model consists of identifying the error profiles of various estimators and the physical parameters of the underlying problem and designing the fusers for combining the individual estimators. Two types of information fusers were used in fuser model development, namely, linear fuser and near neighbor projective fuser.

Initially, we combined the statistical and deterministic estimators using the linear fuser, which is a special case of the isolation fusers [21]. The isolation fusers are shown to perform probabilistically as good as best estimator [5,21]. Given  $n$  estimators,  $f_1(x), \dots, f_n(x)$ , the linear fuser is given by  $f(x) = w_1 f_1(x) + \dots + w_n f_n(x)$ , where  $w_1 \dots w_n$  are the weights. We computed the weights for the fuser by minimizing the error of the fuser for the training set.

The projective fuser [9] based on the nearest neighbor concept was also implemented in the study. This fuser partitions the space of domain  $X$  into regions based on the nearest to the sample. For each region an estimator with the lowest empirical error is used to compute the function estimate for all points in the region. This fuser is easy to implement and provides finite-sample performance bounds under fairly general smoothness or non-smoothness conditions on the individual estimator.

The program was written in C where the solution is based on solving a quadratic programming problem. In this study, we utilized the linear fuser and near neighbor projective fuser to develop the embrittlement models, six parameters, namely, Cu, Ni, P, fast fluence, irradiation time, and irradiation temperature, were incorporated into model development. Eight different models were investigated including four neural network models, two ORNL models, the K-nearest neighbor regression method, and the Eason's model.

*ORNL Fuser Model I* – Linear Fuser was implemented into Fuser Model I development. The results of the linear fuser model indicate that this newly developed embrittlement model has about 56.5% and 32.8% reductions in uncertainties for GE BWR base and weld data, respectively, compared to that of Reg. Guide 1.99, Rev. 2. These are substantial improvements on the embrittlement predictions for the reactor pressure vessel steels. The plots of information model residual and its two-sigma uncertainties for base and weld materials are illustrated in Figs. 13-14, respectively.

*ORNL Fuser Model II* – Fuser Model II is a simplified version of Fuser Model I, excluding the irradiation temperature from the fitting parameter and excluding the Eason's model from the fusion modeling. The data scatter of residuals for Fuser Model II are essentially the same as that of Fuser Model I. The results of ORNL Fuser Model II indicate that it has about 55.2% and 28.8% reduction in uncertainties for GE BWR base

and weld data, respectively, compared to that of Reg. Guide 1.99, Rev. 2's model. This indicates that fuser model I has marginal improved performance compared to that of fuser model II. Thus, the impact of irradiation temperature on embrittlement modeling for the GE BWR surveillance data can be considered as secondary.

*ORNL Fuser Model III* – Near neighbor projective fuser was implemented in Fuser Model III development. The results of the projective fuser model indicate that it has about 67.3% and 52.4% reductions in uncertainties for GE BWR base and weld data, respectively, compared to that of Reg. Guide 1.99, Rev. 2. These are significant improvements on the embrittlement predictions for the reactor pressure vessel steels. The plots of information model residual and its two-sigma uncertainties for base and weld materials are illustrated in Figs. 15-16, respectively.

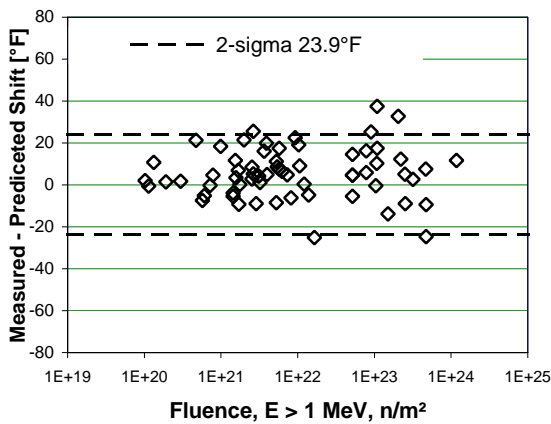


Fig. 13. Fuser Model I base residuals.

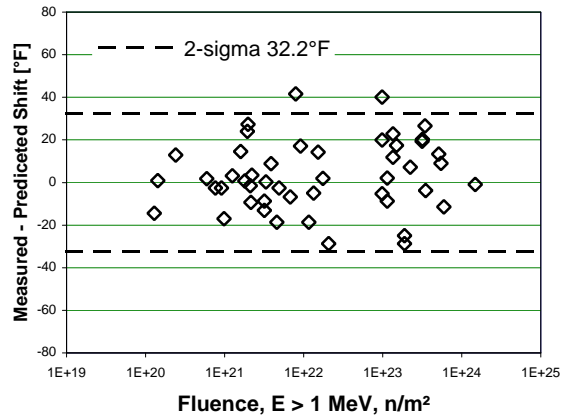


Fig. 14. Fuser Model I weld residuals.

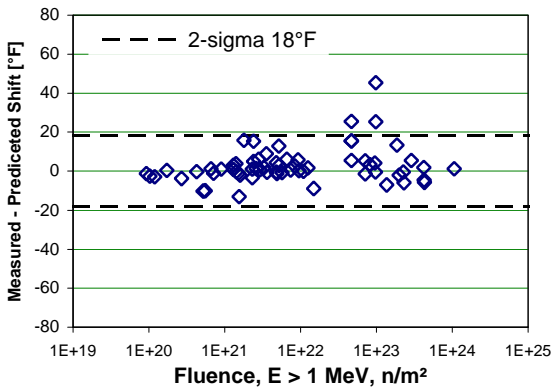


Fig. 15. Fuser Model III base residuals.

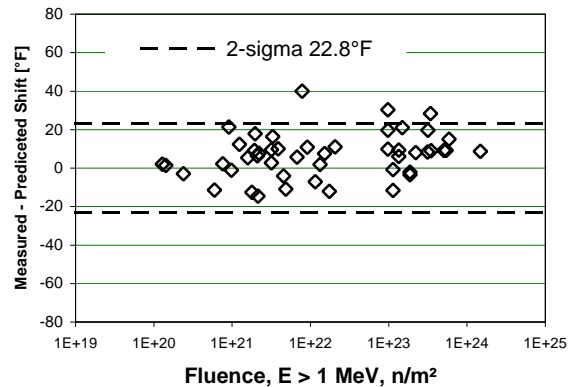


Fig. 16. Fuser Model III weld residuals.

## Discussion

The comparison of the performance of the embrittlement models, based on the two-sigma uncertainty of residual values, is stated in Table 1. The Fuser Model III gave the best performance among all the embrittlement prediction models. ORNL embrittlement

Table 1 - *Two-sigma uncertainty of the embrittlement models for GE BWR data.*

Embrittlement model	Parameters					Two sigma of residual (°F)	
	Cu	Ni	$\phi t$	$t_i$	$T_c$	Base (64 points)	Weld (48 points)
Reg. Guide 1.99, Rev. 2	x	x	x			55.0	47.9
ORNL Fuser Model I	x	x	x	x	x	23.9	32.2
ORNL Fuser Model II	x	x	x	x		24.6	34.1
ORNL Fuser Model III	x	x	x	x	x	18.0	22.8
ORNL Model I	x	x	x			39.6	41.8
ORNL Model II	x	x	x	x		27.6	38.5
Eason's Model	x	x	x	x	x	40.9	51.0
K-NNR Model	x	x	x	x	x	39.1	41.4
ANN-4 Model	x	x	x	x	x	56.4	78.8*

\*| Residual | > 100°F are not included in two-sigma uncertainty evaluation.

models indicate that ORNL Model II is superior to ORNL Model I by including irradiation time to simulate fluence-rate effect. Thus, the implication of a flux effect in BWR environment was revealed in the model development.

The authors would like to point out that the fusion modeling developed here is based on GE BWR data, including 110 available sample data, where, Reg. Guide 1.99/R2 and Eason's Model were developed based on both PWR and BWR surveillance data. Thus, the superior prediction by ORNL Fusion model compared to that of Reg. Guide 1.99/R2 and Eason's models may be partially due to the subset of power reactor data used in the model development. However, by the same token, this study may also demonstrate the superiority and advantage of using subset data, for example, the vendor specific data, to develop power reactor embrittlement models. (The reason is explained in the next paragraph.) In general a large data set with similar characteristics or controllable parameters will generate a better trend prediction compared to its subset. But a misleading trend curve can result from a large data set built upon different bases and uncontrollable parameters, revealed by its large uncertainty.

The R.G. Guide 1.99/R2 was formulated based on Guthrie's model and Odette's model and no temperature effect was considered in embrittlement model development, where, the fluence factor (FF) and plates' chemistry factor (CF) are from Guthrie's model [18]. 177 surveillance data were used in Guthrie's model development, however, only 6 data are from BWR environment. Thus, BWR surveillance data may not be properly characterized from Reg. Guide 1.99/2's model. From ASTM E10.02 database, the mean temperature and one standard deviation of BWR and PWR data are  $540.3 \pm 13.6^\circ\text{F}$  and  $545.7 \pm 10.4^\circ\text{F}$ , respectively. Therefore, from the irradiation temperature variability point, the sample temperature environment of PWR and BWR are comparable. Currently, there are four major commercial power reactor vendors in the U.S., namely, Westinghouse, General Electric, Babcock & Wilcox, and Combustion Engineering. Each vendor has its unique designs and specific operating procedures. There are significant

problems associated with insufficient information, such as the detailed irradiation temperature of surveillance specimen and the thermal gradient within surveillance capsules, and the lack of data in particular regions of interests to characterize the vendor's service environments. About 64% of PR-EDB data is from Westinghouse; thus, the trend curve of all the four vendors' data will closely resemble the Westinghouse reactor environment. Furthermore, B&W surveillance data appears to experience higher irradiation temperature (based on capsule melting wire) compared to other vendors., Combining low- and high-temperature data may bring further bias on top of bias from the modeling point. For example, from the trend curve of all the vendor data, the high irradiation temperature data shows negative bias (i.e. prediction model shows over-prediction) and low irradiation temperature data show positive bias. However, the overall bias (or uncertainty) will cancel each other resulting in a misleading statistical outcome, such as means and uncertainty.

Eason's model covers both PWR and BWR environment, where 96 BWR data were included in model development and coolant inlet temperatures were incorporated into governing equations to simulate temperature effect. In practice the coolant inlet temperature is incorporated into the embrittlement model to simulate the irradiation temperature for a pressurized light-water reactor. However, a past study [11] showed that a large bias can still be identified in Eason's model for surveillance data from a higher irradiation temperature environment and the bias is similar to that of Regulatory Guide 1.99, Rev. 2 [18]. This may indicate that the coolant inlet temperature is not equivalent to the irradiation temperature experienced by the surveillance specimens. Furthermore, from this study on fuser models, neither including or excluding coolant inlet temperature has a significant impact on the trend curve, which may further support the above statement.

For surveillance data, significant deviations of the measured shift from the trend curve (i.e., more or less than 34°F for plate materials) should be considered as a warning flag pointing to a possible anomalous capsule environment. The large uncertainties are the result of errors in the overall environment description. But, limited attention has been given to characterizing the irradiation temperature environment of the surveillance specimens. In general, the neutron environment, fluence and flux, can be determined fairly accurately and possible effects from these sources are relatively small in a power reactor environment. However, the temperature of surveillance capsules environments still heavily rely on the measurement of the melting wire. A more detailed analytical investigation of specimen temperature is needed based on detailed neutronic and thermal-mechanical analysis for specific capsule and specimen loading configuration, to facilitate the RPV surveillance program in confidence. Thus, in the current trend curve development, the most likely reason for deviations from the trend curve is the specimen temperature.

To develop a global embrittlement model for U.S. power reactors an independent investigation of each subgroup (each vendor) is recommended. Upon completing the investigations, if substantial improvement is achieved for each subset based on the proposed methodology, then an information fusion technique will be utilized to integrate all the subset models into a global RPV embrittlement model.

## **Conclusions**

A new methodology that incorporates the chemical compositions into the Charpy trend curve was developed. The purpose of this new fitting procedure is to generate a new multi-space topography that can properly reflect the inhomogeneity of the surveillance materials and utilize this multi-space trend surface to link and project the surveillance test results to that of reactor pressure vessel steels. Furthermore, based on this new approach, the new advanced fitting procedure achieves a reduction in uncertainty by 27%, compared to that of conventional hyperbolic tangent fit procedure.

We described an information fusion method for the embrittlement prediction in light water reactor pressure vessels by combining domain models with neural networks, and nearest neighbor regressions. Our method resulted in 67.3% and 52.4% reduction in 2-sigma uncertainties compared to that of the Reg. Guide 1.99, Rev. 2's model for base and weld materials, respectively. This new approach combines the conventional non-linear methods and model-based methods into an integrated methodology applicable for modeling material aging processes. This approach can potentially assist the nuclear industry on the issues of safety and lifetime extension of aging commercial nuclear power plants. By using a wide spectrum of methods, the proposed tool can potentially handle the subtle non-linearities and imperfections and serve as a calibration and benchmark for the existing models. The predictions generated by our system have the potential for providing efficient, reliable, and fast results, and can be an essential part of the overall safety assessment of material aging research.

Future improvements of the proposed method can be made using the k-fold cross validation method [22]. In this method data is partitioned into k blocks, of which k-1 of them are used as the training set and the remaining as the test set. This process is repeated for all k permutations of choosing the k-1 blocks for the training set. Thus, at the end of this exercise there are k accuracy estimates in terms of the average of test and training error. Using these k estimates we compute the average accuracy, variance and the confidence interval. Based on the results, one can assign weights to various blocks in proportion to test error. These weights will then be used in developing an i-neighbor version of the proposed fuser. More generally, the cross validation method can also be used to compare various methods in a statistically informative manner.

## **Acknowledgements**

The authors gratefully acknowledge the efforts of R. K. Nanstad for his valuable comments on this research. This research is sponsored by the R&D Seed Money Program of Oak Ridge National Laboratory, and by Engineering Research Program Office of Basic Energy Sciences of U.S. Department of Energy, under contract DE-AC05-00OR22725 with UT-Battelle, LLC.

## **References**

- [1] J.A. Wang, Embrittlement Data Base, Version 1, NUREG/CR-6506 (ORNL/TM-13327), U.S. Nuclear Regulatory Commission, August 1997.



- [2] N.S.V. Rao, Multiple sensor fusion under unknown distributions, *Journal of Franklin Institute*, 1999, vol. 336, no.2, pp. 285-299.
- [3] Wang, J. A., "Analysis of the Irradiation Data for A302B and A533B Correlation Monitor Materials," NUREG/CR-6413, ORNL/TM-13133, 1996.
- [4] N.S.V. Rao, Multisensor fusion under unknown distributions: Finite sample performance guarantees, in *Multisensor Fusion*, A.K. Hyder (editor), Kluwer Academic Publishers, 2001.
- [5] N.S.V. Rao, On fusers that perform better than best sensor, *IEEE Transactions on Pattern Analysis and Machine Intelligence*, vol. 23, no. 8, 2001, pp. 904-909.
- [6] R.O. Duda, P. E. hart, and D. G. Stork, *Pattern Classification*, John Wiley and Sons, Second Edition 2001.
- [7] N.S.V. Rao, V. Protopopescu, On PAC learning of functions with smoothness properties using feedforward sigmoidal networks, vol. 84, no. 10, *Proceedings of IEEE*, 1996, pp.1562-1569.
- [8] J.A. Wang, "Development of Embrittlement Prediction Models for U.S. Power Reactors." *Effect of Radiation on Materials: 18th International Symposium*, ASTM STP 1325, American Society for Testing and Materials, Philadelphia, pp.525-540, March 1999.
- [9] N. S. Rao, "Nearest Neighbor Projective Fuser for Function estimation," Proc. Conf. On Information Fusion, 2002.
- [10] L.K. Mansur, "Mechanisms and Kinetics of Radiation Effects in Metals and Alloys," *Kinetics of Nohomogeneous Processes*, ed. by Gorden R. Freeman, 1987.
- [11] J.A. Wang, "Analysis of the Irradiated Data for A302B and A533B Correlation Monitor Materials," *Effect of Radiation on Materials: 19th International Symposium*, ASTM STP 1366, American Society for Testing and Materials, Philadelphia, pp. 59-80, March 2000.
- [12] J.A. Wang, F. B. K. Kam, and F. W. Stallmann, "Embrittlement Data Base (EDB) and Its Applications," *Effects of Radiation on Materials: 17th Volume*, ASTM STP 1270, American Society for Testing and Materials, Philadelphia, pp. 500-521, August, 1996.
- [13] G.L. Guthrie, Charpy Trend Curves Based on 177 PWR Data Points, NUREG/CR-3391, U.S. Nuclear Regulatory Commission, 1983.
- [14] G.R. Odette, P.M. Lombrozo, J.F. Perrin, and R.A. Wullaert, "Physically Based Regression Correlations of Embrittlement Data From Reactor Pressure Vessel Surveillance Programs," EPRI NP-3319, Electric Power Research Institute, 1984.
- [15] S.B. Fisher, and J.T. Buswell, "A Model for PWR Pressure Vessel Embrittlement," Berkeley Nuclear Laboratories, Central Electric Generating Board, GL139PB, 1986.
- [16] A.L. Lowe, Jr., and J.W. Pegram, "Correlations for Predicting the Effects of Neutron Radiation on Linde 80 Submerged-Arc Welds," BAW-1803, Rev. 1, May 1991.
- [17] C. Brillaud, F. Hedin, and B. Houssin, "A Comparison Between French Surveillance Program Results and Predictions of Irradiation Embrittlement," Influence of Radiation on Material Properties, ASTM STP 956, 1987, pp. 420-447.
- [18] P.N. Randall, "Basis for Revision 2 of the U.S. Nuclear Regulatory Commission's Regulatory Guide 199," *Radiation Embrittlement of Nuclear Reactor Pressure Vessel Steels: An International Review (Second Volume)*, ASTM STP 909, 1986, pp. 149-162.
- [19] E. D. Eason, J. E. Wright, and G. R. Odette, Improved Embrittlement Correlations for Reactor Pressure Vessel Steels, NUREG/CR-6551, U.S. Nuclear Regulatory Commission, 2000.
- [20] M.H. Hassoun, *Fundamentals of Artificial Neural Networks*, MIT Press, 1995.
- [21] N.S.V. Rao, Finite sample performance guarantees of fusers for function estimators, *Information Fusion*, vol. 1, no. 1, 2000, pp. 35-44.
- [22] R. O. Duda, P. E. Hart, and D. G. Stork, *Pattern Classification*, John Wiley and Sons, 2001, second editon.